Mon. Not. R. Astron. Soc. **275**, 1171–1184 (1995)

Radio source asymmetries and unified schemes

P. N. Best, D. M. Bailer, M. S. Longair and J. M. Riley
Cavendish Laboratory, Madingley Road, Cambridge CB3 0HE

Accepted 1995 March 16. Received 1995 March 16; in original form 1994 August 2

ABSTRACT

The angular asymmetries and relative separations of the hotspots of Fanaroff–Riley II (FRII) radio sources in a complete sample of 3CR sources have been used to study the effects of misalignment of the directions of ejection and the velocities of the hotspots. It is found that the observed distribution of asymmetry angles is consistent with unified schemes for radio galaxies and radio quasars and with the source components being ejected uniformly within an angle $\phi_{\max}$ of 6°–7° about the source axis. The separation quotients of the hotspots are also consistent with unified schemes, if the velocities of the hotspots have a broad distribution about a mean of $0.2c$, with values extending at least up to $0.4c$.

Key words: galaxies: active – galaxies: jets – quasars: general – radio continuum: galaxies.

1 INTRODUCTION

Barthel has listed a number of convincing reasons for supposing that powerful radio galaxies and radio quasars are the same objects viewed at different angles to the line of sight (Barthel 1989, 1994). According to his unified scheme, those radio sources with axes oriented within an angle of roughly 45° to the line of sight are observed to be quasars, while those close to the plane of the sky are classified as radio galaxies. This model provides a natural explanation for the large percentage of quasars that have one-sided jets and for the fact that quasars appear systematically smaller than radio galaxies. It has been suggested that the nuclear regions of these sources are surrounded by dusty tori of obscuring material which, in radio galaxies, prevents the observation of central broad-line regions that are clearly visible in quasars.

The availability of large numbers of radio maps of powerful radio sources with very high angular resolution has enabled further tests of Barthel's hypothesis to be carried out. If quasars are truly oriented along the line of sight then various observed asymmetries should appear more pronounced in that population than in the radio galaxies. In this paper we present an analysis of two such asymmetries: the separation quotients and the asymmetry angles. In Section 2 we describe the data base used in the analysis. Section 3 is a discussion of separation quotients and the fractional separation differences; the data are analysed in Section 4. In Section 5 we consider the distribution of asymmetry angles. The effect of this analysis upon the separation quotients is discussed in Section 6. In Section 7, the correlations of the two asymmetries are presented, and the conclusions are discussed in Section 8.

2 THE NEW DATA BASE

The new data base consisted initially of the revised complete sample of 3CR radio sources at declinations $|\delta| \geq 10°$ defined by Laing, Riley & Longair (1983, hereafter LRL). A literature search was made for maps of all the sources in this sample (Bailer 1993), supplemented by new Very Large Array (VLA) observations which have been obtained recently by us (Best et al., in preparation). The analysis of source asymmetries and separation quotients was restricted to those FRII sources in which hotspots could be clearly defined towards the extremities of both components. In cases in which more than one hotspot was observed in a source component, the more distant hotspot was selected. Of the 126 FRII sources, 95 had well-defined hotspots in both components. In most cases, the nucleus was defined by a central radio component; where no central radio component was detected, the centre of the optical image of the galaxy or quasar was used to define the position of the nucleus. Of the 95 sources, 23 were quasars and 72 were radio galaxies. For comparison, among the 126 FRII sources, there were 29 quasars and 97 radio galaxies. All 95 radio sources were of high radio luminosity, $P_{178} \geq 2.0 \times 10^{26}$ W Hz^{-1}, and constituted a representative sample of the FRII sources in the complete 3CR sample. In all our computations, Hubble's constant has been taken to be 50 km s^{-1} Mpc^{-1} and the deceleration parameter $q_0 = 0.5$.

The data used in the analysis are presented in the Appendix as Table A1. The quantities derived from the radio maps were the separation quotient Q, defined as the ratio $Q = \theta_1/\theta_2$, where θ_1 and θ_2 are the angular distances from the nucleus of the more distant and closer hotspots,

respectively, and the asymmetry angle ζ, which was taken to be 180°, minus the observed angle between vectors drawn from the nucleus of the radio source to the hotspots. The values of ζ typically lie between 0° and 20°. Of the 95 sources, 86 were common to the sample of McCarthy, van Breugel & Kapahi (1991) who studied correlations between radio and optical asymmetries. The majority of the estimates of the separation quotients were in agreement within about ± 0.1, but there were 11 cases in which significant discrepancies were found. These cases are discussed in the Appendix and the adopted values justified.

3 THE ANALYSIS OF SEPARATION QUOTIENTS

The separation quotient $Q=\theta_1/\theta_2$ for complete samples of FRII sources can be used to set upper limits to the velocities of advance of the hotspots through the intergalactic gas. It is assumed that the two hotspots have moved at the same speed, v, in opposite directions from the nucleus. As shown by Ryle & Longair (1967) and Longair & Riley (1979), if θ is the angle between the axis of the source and the line of sight to the observer, the separation quotient is $Q=\theta_1/\theta_2=(1+\beta\cos\theta)/(1-\beta\cos\theta)$, where θ_1 and θ_2 are the angular distances of the hotspots more distant from and closer to the nucleus, respectively, and $\beta=v/c$. If the angles between the axes of the sources and the line of sight are randomly distributed, the probability distribution of Q is

$$p(Q)=\frac{2}{\beta(Q+1)^2}\,\mathrm{d}Q,$$

from $Q=1$ to a maximum value $Q=(1+\beta)/(1-\beta)$. Longair & Riley (1979) found that, for a complete sample of FRII sources from the 3CR catalogue, the distribution $p(Q)$ was remarkably narrow and an upper limit to the average velocity of the hotspots of $\beta\approx 0.2$ was derived.

Banhatti (1980) suggested that a better procedure was to use the statistic $x=(Q-1)/(Q+1)=(\theta_1-\theta_2)/(\theta_1+\theta_2)$ which he called the *fractional separation difference*. In this case, $x=\beta\cos\theta$. For a random distribution of angles, x is uniformly distributed between $x=0$ and $x=\beta=v/c$, that is, $p(x)\,\mathrm{d}x=(1/\beta)\,\mathrm{d}x$. The probability distribution for x has an advantage over that for Q in that it allows easy determination of the probability distribution of the velocities of the hotspots. If $P(x)$ is the observed probability distribution of x in a complete sample of sources, the distribution of velocities can be found by summing a series of distributions $p(x)$ for different values of $\beta=v/c$ with appropriate weightings. The probability distribution $g(\beta)$ of sources having velocity $v=\beta c$, can be found by differentiating the function $P(x)$, since it is apparent that

$$P(x)=\int_{\beta=x}^{\beta=1}\frac{g(\beta)}{\beta}\,\mathrm{d}\beta. \qquad (1)$$

Banhatti used this procedure to show that the velocity distribution of the source components was quite broad with an average velocity of about 0.2, assuming the model to be a correct description of the dynamics of the sources.

We have analysed the properties of the distributions of the separation quotients and fractional separation differences using our new data base to investigate whether there is any evidence for significantly relativistic hotspot velocities.

4 DISTRIBUTION OF FRACTIONAL SEPARATION DIFFERENCES

Fig. 1 shows the probability distribution $P(x)$ for the 95 sources in the sample, the quasars being distinguished from the radio galaxies. There is a clear tendency for the radio galaxies to have smaller values of x than the quasars. It is particularly noticeable that there are few quasars with values of $x\leq 0.1$, whereas the radio galaxy distribution shows a pronounced maximum at $x=0$. The mean value of x for the quasars is greater than that for the radio galaxies, the values being $\bar{x}_{\mathrm{Q}}=0.206\pm0.031$ and $\bar{x}_{\mathrm{RG}}=0.124\pm0.013$. Application of a Mann–Whitney U-test to the two data sets shows that the hypothesis that the sources are drawn from the same (unknown) parent sample is rejected at the 99 per cent confidence level.

A natural explanation of this difference between the values of $\bar{x}$ for radio galaxies and quasars is to associate it with relativistic motion of the hotspots, as described by the simple model of Section 3. If the axis of the source is observed at a small angle to the line of sight, a quasar is observed and large values of $x=\beta\cos\theta$ are expected. If the angle of the axis of the source to the line of sight is large, the source is identified as a radio galaxy and will appear much more symmetrical. Only if the velocities of the components are non-relativistic, $\beta\lesssim 0.1$, are symmetric quasars observed.

To test this picture, the velocity distribution of the hotspots $g(\beta)$ has been determined using Banhatti's procedure. By inspection it can be seen that a function of the form $P(x)=(A+1)(1-x)^A$ satisfies the boundary conditions $\int P(x)\mathrm{d}x=1$ and $P(x)=0$ at $x=1$, and also provides a satisfactory fit to the data if $A=5.3$ (Fig. 2a). The corresponding velocity distribution $g(\beta)$, derived by differentiation of $P(x)$ according to the prescription of equation (1), is shown in Fig. 2(b). As noted by Banhatti, the velocity probability distribution extends to large velocities and so the fact that there is one quasar with $x=0.74$ and one radio galaxy with $x=0.53$ is not as anomalous as it might appear from Fig. 1.

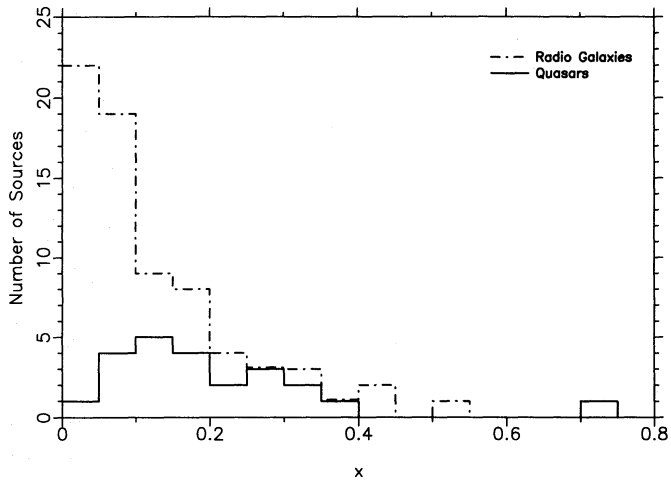

Figure 1. The distribution of the fractional separation differences for 95 3CR radio sources, comprising 23 quasars and 72 radio galaxies.

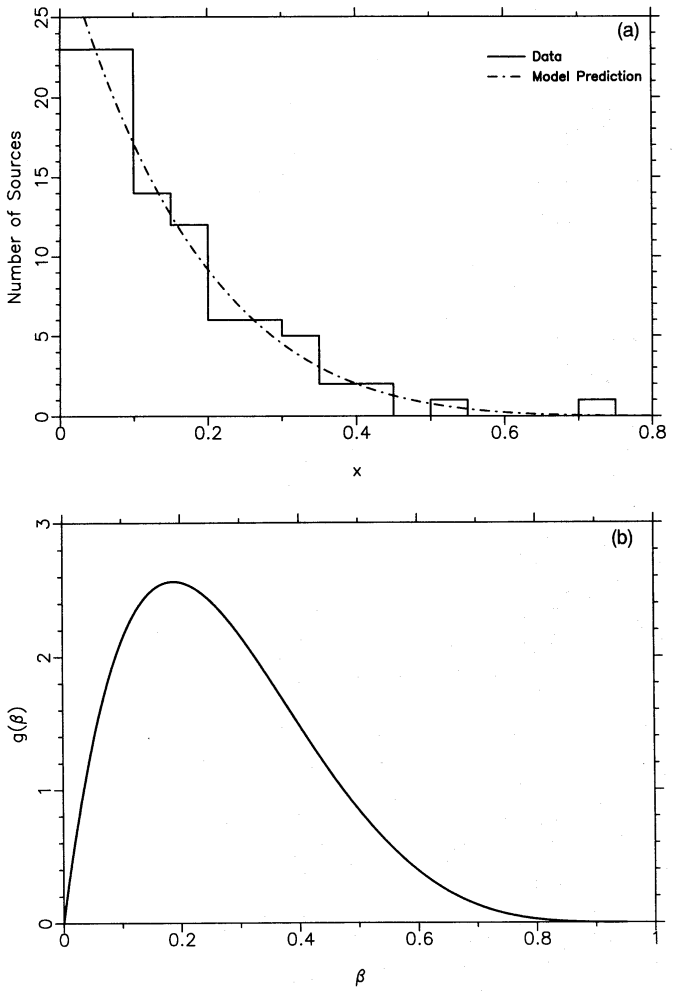

Figure 2. (a) The fit of the function $P(x)=6.3(1-x)^{5.3}$ to the observed distribution of $P(x)$. (b) The probability distribution $g(\beta)$ is found by differentiating $P(x)$ as described in Section 3.

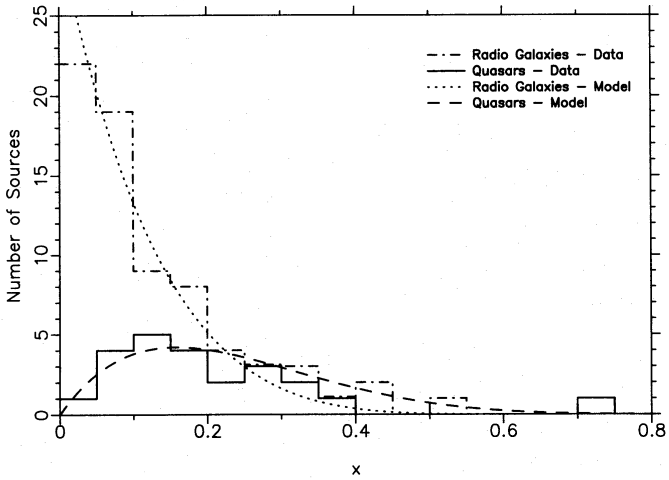

Figure 3. Comparison of the observed and predicted distributions $P(x)$ for radio galaxies and quasars for the velocity distribution shown in Fig. 2(b).

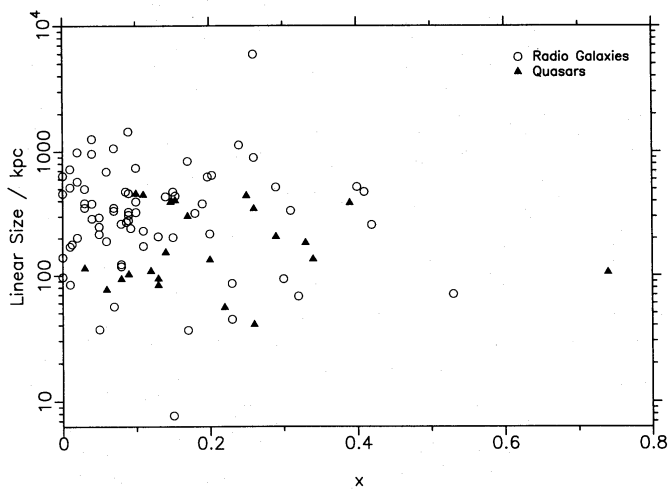

Figure 4. A plot of the linear size of the radio source against fractional separation difference x.

From the distribution $g(\beta)$, it is straightforward to work out the predicted distributions $P(x)$ for the radio galaxies and quasars, according to Barthel's model. We adopt a dividing angle between the quasar and radio galaxy populations of 45° to the line of sight. The comparison between the observed and predicted distributions is illustrated in Fig. 3, from which it can be seen that there is remarkable agreement between the expectations of the model and the observed $P(x)$ distribution for both the quasars and the radio galaxies. This provides strong support not only for unification schemes, but also for mildly relativistic advance of the hotspots. Indeed, if the source velocities were non-relativistic, some other astrophysical reason would have to be found to explain why, despite the convincing evidence for the unified picture of radio galaxies and quasars, the quasars are systematically more asymmetric than the radio galaxies.

It is not surprising that the model is also consistent with the observation that the physical sizes of the quasars are systematically smaller than those of the radio galaxies, since this was part of Barthel's original argument, using essentially the same data base. For a dividing angle of 45°, it is expected that the ratio of the average physical size of the quasars to that of the radio galaxies would be 1.87. The average sizes of the quasars and radio galaxies in the samples are 207 ± 29 and 391 ± 35 kpc, respectively, in the latter case omitting the giant source 3C 236 which has physical size 6 Mpc. If 3C 236 were included, the latter figure would be 465 ± 81 kpc. The observed ratio of physical sizes is thus 1.89 (it would be 2.25 if 3C 236 were included). The correlation between projected (or observed) physical size D and x is displayed in Fig. 4. There is a clear tendency for the quasars to be displaced towards the bottom right of the distribution, although there are a few radio galaxies in the regions populated by the quasars.

One consequence of the relativistic hotspot model, noted by Fokker (1986), is that, as the angle to the line of sight decreases, the value of x increases and the projected physical size of sources of the same intrinsic size decreases. Thus an inverse correlation is expected between observed linear size and the value of x. Fokker found no evidence for such a correlation. The data in Fig. 4 can be used to repeat this analysis; they are of higher quality than those available to Fokker and a number of our values of x and Q differ from those used in his analysis. Application of a Spearman rank

test to our data shows that, at best, there is a weak inverse correlation between x and D, the correlation coefficient being -0.07, significant at only the 75 per cent confidence level. The expected correlation is, however, weakened because of the dispersions in both the physical sizes and inferred velocities of the sources. To estimate the importance of these dispersions, a series of simulations was carried out in which the velocities of the source components were selected at random from the distribution shown in Fig. 2(b) and the intrinsic physical sizes D_0 of sources were selected at random from a uniform distribution, ranging from 100 to 1000 kpc. A typical example of the simulated distributions is shown in Fig. 5, the quasars and radio galaxies being distinguished as in Fig. 4. It can be seen that the expected correlation has been greatly weakened by the intrinsic dispersions in physical size and β but the correlation coefficient is still -0.27, corresponding to a significant inverse correlation at the 3σ confidence level. It is apparent, however, that Figs 4 and 5 show the same qualitative features. The strength of the inverse correlation would be weakened further if, for example, the sources with the highest velocities had greater physical sizes. In fact, our simulations show that, if the intrinsic physical size were proportional to β, a positive correlation coefficient of $+0.20$ would be expected. Thus only a weak intrinsic correlation between D_0 and β is needed to eliminate the expected inverse correlation between D and x.

To test for possible selection effects, the values of x have been plotted as a function of radio luminosity in Fig. 6. It can be seen that the quasars tend to lie towards the upper end of the luminosity range, and in particular that there are no quasars at the lowest luminosities. This corresponds to the fact that, for a flux-limited sample, luminosity is strongly correlated with redshift and that there are no quasars with redshifts $z < 0.3$ in the 3CR sample. Although the quasars tend to lie at higher luminosities than the radio galaxies, it is clear from Fig. 6 that there is no trend *within* either the radio galaxy or quasar populations for x to be correlated with luminosity. Indeed, within the quasar population there is even some evidence for a negative correlation of x with luminosity at the 97 per cent confidence level. We have divided both the radio galaxy and quasar samples into equal high- and low-redshift samples and a comparison of the average values of x for the two classes of object in the two redshift ranges is given in Table 1. There is no statistical difference between the value of $\bar{x}$ in the low- and high-redshift samples of the radio galaxies; the quasars in the lower redshift bin are slightly more asymmetric than those at higher redshift, but only at the 2σ level. This is partially due to the single quasar with $x = 0.74$ falling into this bin. As a final test, the above analysis can be repeated using only those radio galaxies with a redshift of $z > 0.3$, to provide a sample with a luminosity spread equivalent to that of the quasars. For this new sample of 42 galaxies, the average value of x is $\bar{x}_{RG} = 0.135 \pm 0.019$ (compared with $\bar{x}_{RG} = 0.124 \pm 0.013$ for all the radio galaxies) and the distribution of x is remarkably similar to that of the complete sample of 72 radio galaxies. It is apparent, therefore, that the reason that the quasars appear more asymmetric than the radio galaxies is not due to any luminosity or redshift effect.

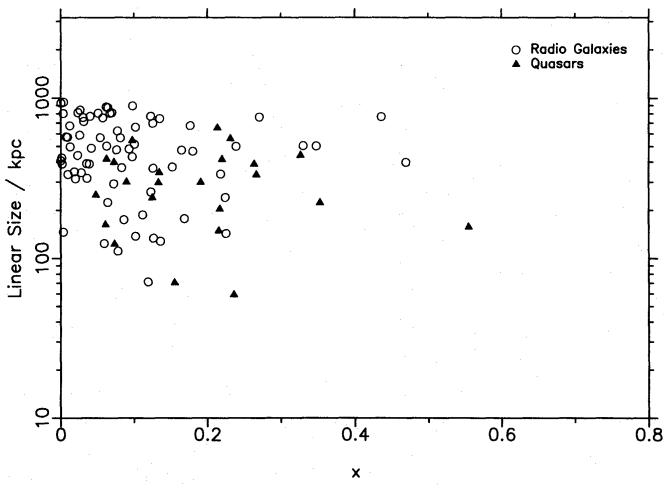

Figure 5. A simulation of the predicted x–D diagram assuming Barthel's unified scheme for radio galaxies and quasars. It is assumed that the hotspots have the velocity distribution shown in Fig. 2(b) and that, intrinsically, their total linear sizes are randomly selected from a uniform distribution covering the range 100 to 1000 kpc.

5 THE DISTRIBUTION OF ASYMMETRY ANGLES ζ

The above analysis of fractional separation differences assumed that the radio sources are linear, whereas this is

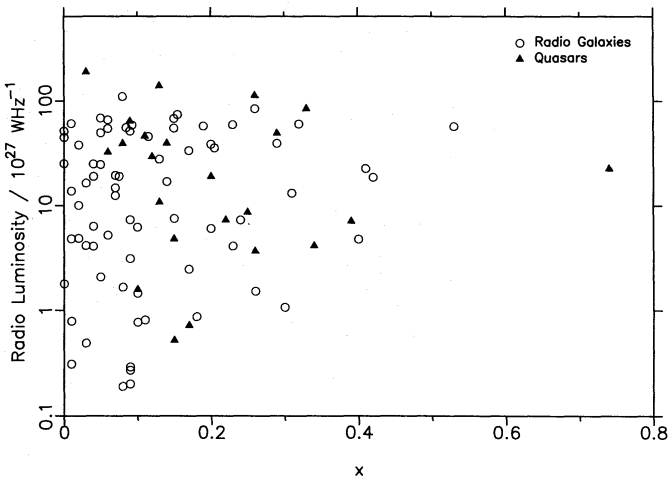

Figure 6. A plot of the radio luminosity against fractional separation difference for the 23 quasars and 72 radio galaxies in the sample.

Table 1. Values of $\bar{x}$ and $\bar{\zeta}$ for radio galaxies and quasars.

Sample	Number of objects	$\bar{x}$	$\bar{\zeta}$
Radio galaxies $z < 0.425$	36	0.113 ± 0.019	5.81 ± 0.83
Radio galaxies $z > 0.425$	36	0.134 ± 0.019	4.69 ± 0.68
Quasars $z < 1.02$	12	0.258 ± 0.051	11.12 ± 3.22
Quasars $z > 1.02$	11	0.149 ± 0.023	12.18 ± 2.82

known not to be the case. Histograms showing the probability distributions of the asymmetry angle ζ for quasars and radio galaxies are displayed in Fig. 7. A range of asymmetry angles is found among both samples, the distribution for the quasars being broader and flatter than that of the radio galaxies. A Mann–Whitney *U*-test shows that the likelihood that the two distributions are drawn from the same parent distribution is less than 1 per cent.

The observed distributions of asymmetry angles for radio galaxies and quasars can, however, be naturally explained if both classes of source belong to the same parent population observed at different angles to the line of sight. To model the non-collinearity, we assume that the hotspots are powered by beams from the nucleus, which are misaligned by an angle ϕ as illustrated in Fig. 8. The source is observed at some unknown angle θ to the line of sight and, for the sake of computational convenience, it is assumed that one component is ejected along the angle θ and that the other lies at an angle ϕ

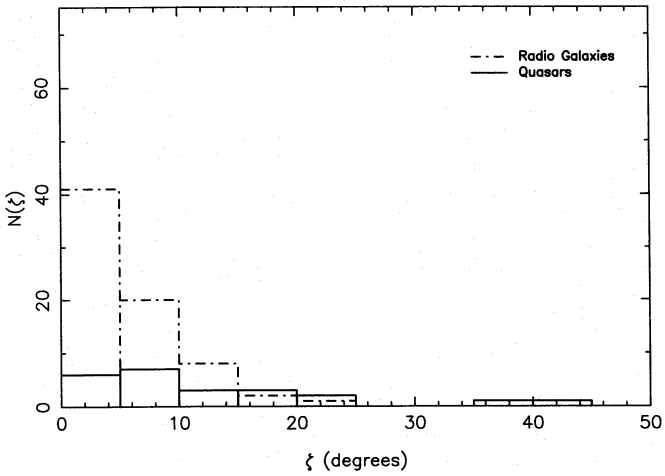

Figure 7. The distribution of asymmetry angles ζ for the radio galaxies (dashed line) and the quasars (solid line) in the complete sample of sources.

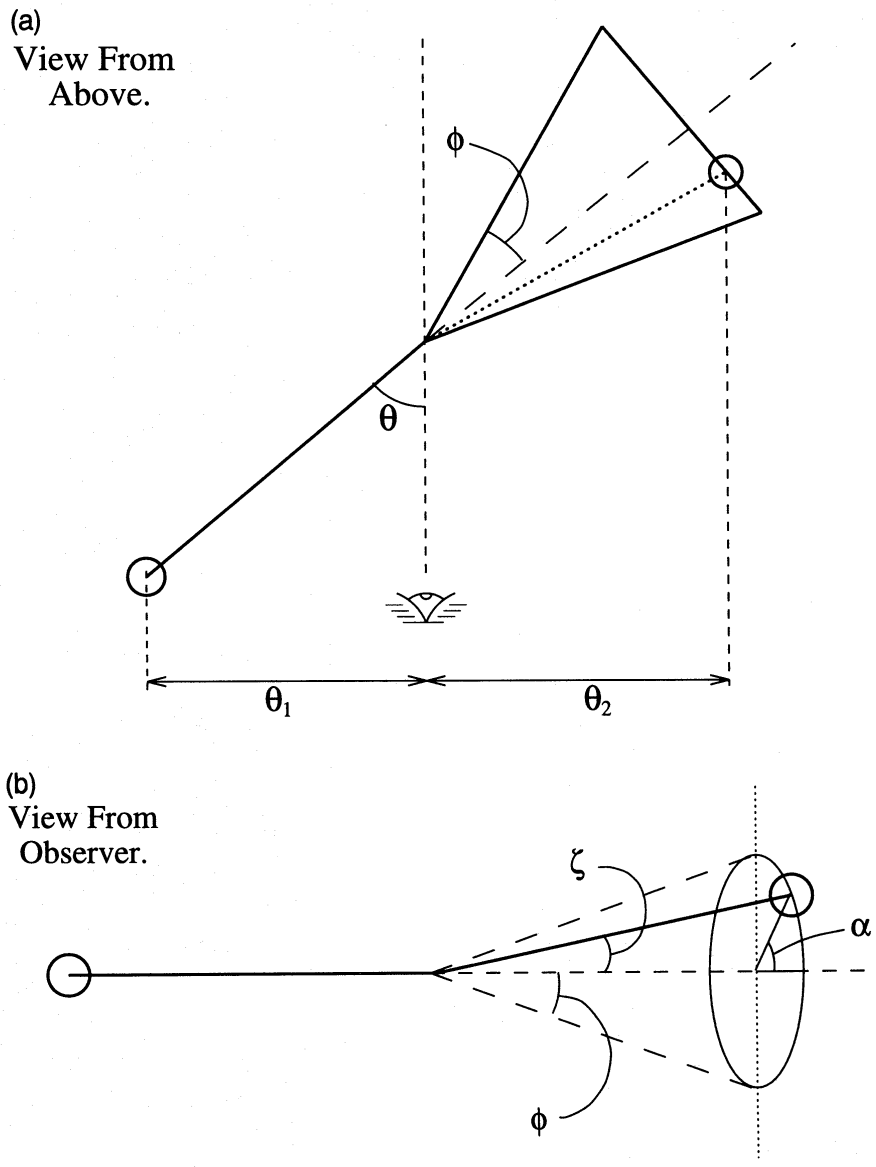

Figure 8. Illustrating the geometry of the simple model for the ejection of the source components at an angle ϕ to the axis of the double source as defined by the angle θ. (a) The view from above; (b) the view from the observer. ζ is the projected asymmetry angle as measured by the distant observer.

to this direction but on the opposite side of the source, as illustrated in the diagram. In our simulations, it is assumed that the second component is ejected at an arbitrary angle within the cone defined by the angle ϕ_{max}, that is, $p(\phi)\mathrm{d}\phi \propto \sin\phi\,\mathrm{d}\phi$. If the second hotspot is at distance r_0 from the nucleus, it must lie on the circle that forms the base of a cone of angle ϕ and height $r_0\cos\phi$. If α is the angle around the cone, measured from $\alpha = 0$ when the two hotspots lie in a plane including the nucleus and the observer, the observed value of ζ is given by

$$\tan\zeta = \frac{\sin\phi\sin\alpha}{\sin\phi\cos\alpha\cos\theta + \cos\phi\sin\theta}.$$

The value of ζ depends only upon the geometry of the source and not upon any assumptions about the dynamics of the hotspots. On the adoption of Barthel's picture, it is assumed that, if the angle θ lies within 45° of the line of sight, the object is classified as a quasar, and, if θ lies in the range 45° to 90°, the object is classified as a radio galaxy.

In Figs 9(a)–(d), the predicted probability distributions of ζ for opening angles ϕ_{max} of 5°, 10°, 15° and 20° are presented. It can be seen that the observed distributions of both radio galaxies and quasars shown in Fig. 7 would be consistent with values of ϕ_{max} of about 10°. Thus the observed distribution of asymmetry angles is consistent with the type of unified scheme for radio galaxies and quasars proposed by Barthel – the quasars show a larger range of asymmetry angles because they are observed closer to the line of sight than the radio galaxies.

These conclusions are consistent with other evidence on correlations between angular asymmetries and other properties of the sources. Kapahi & Saikia (1982) and Hough & Readhead (1989) found that the bending angles of the source components (equivalent to our asymmetry angles) are correlated with the dominance of the radio core, while these authors and Hintzen, Ulverstad & Owen (1983) found an inverse correlation between bending angle and projected linear size. Both sets of observations imply that the axes of sources observed closer to the line of sight are more likely to appear misaligned.

Barthel & Miley (1988) suggested that more distant quasars appear to have more bent, distorted structures than those observed nearby. Kapahi (1990) analysed a better-defined sample and found no evidence for such a difference. We have tested our sample for any evidence of this effect by

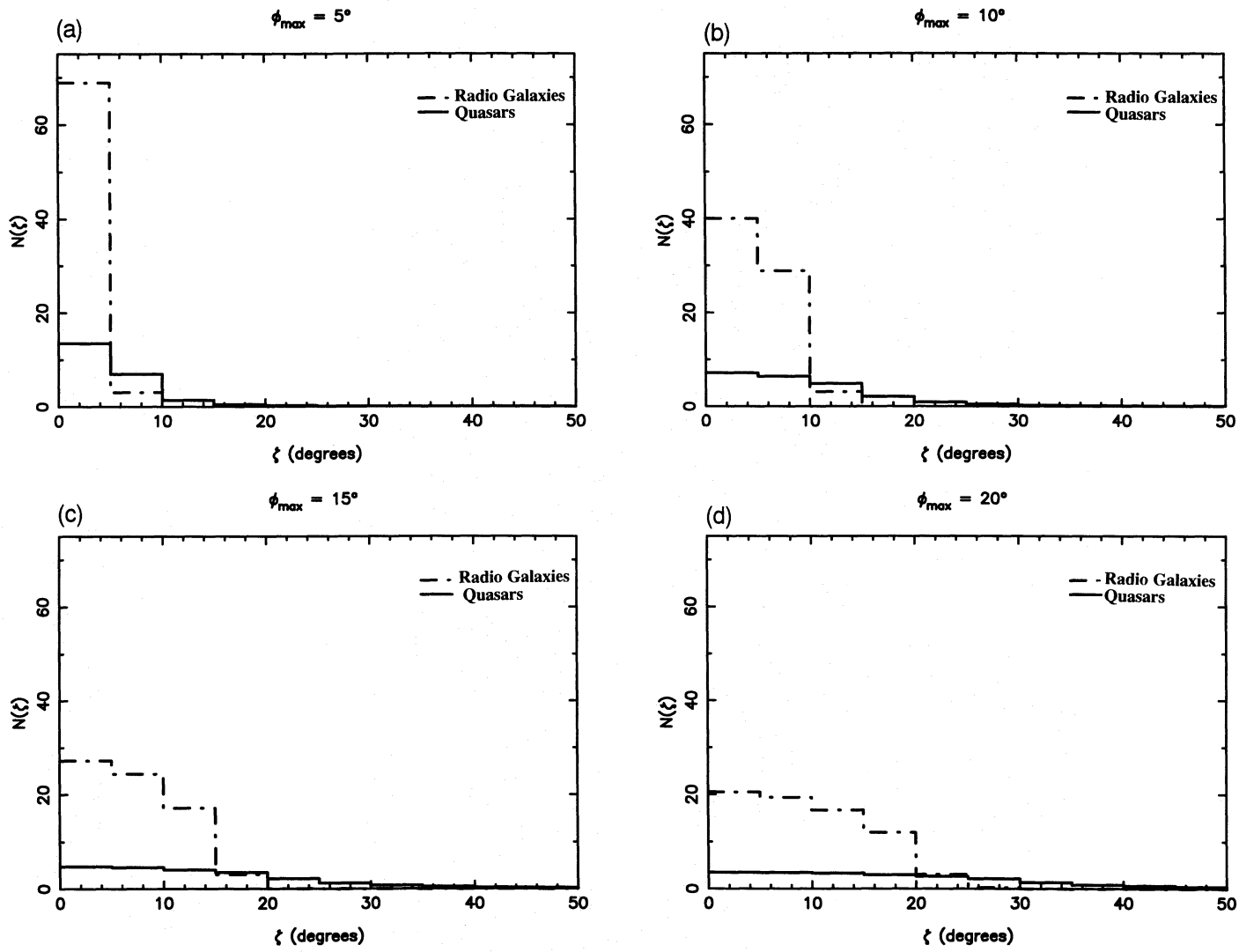

Figure 9. The predicted probability distributions for the angle ζ for different assumed values of ϕ_{max} of (a) 5°, (b) 10°, (c) 15° and (d) 20°.

dividing both the radio galaxy and quasar samples into two redshift bins, and the mean values for each are included in Table 1. There is no evidence for any dependence of the asymmetry angle upon redshift in either sample.

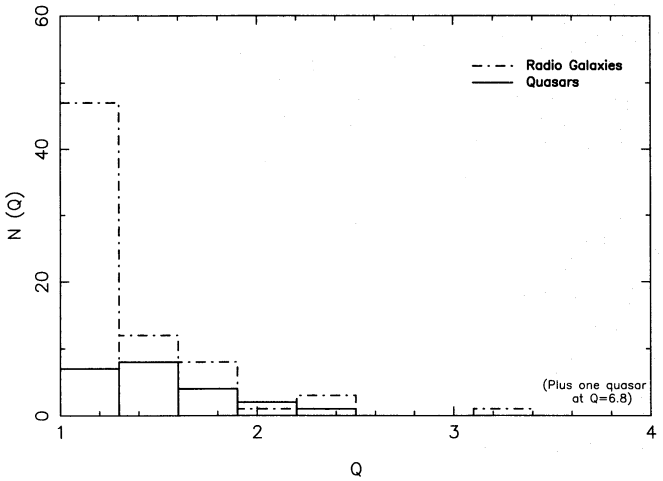

Figure 10. The observed distribution of the separation quotient Q for the sources in the sample.

6 ASYMMETRY ANGLES AND THE INTERPRETATION OF THE SEPARATION QUOTIENTS

In the interpretation of the distribution of x in terms of mildly relativistic motion of the hotspots in Section 3, it was assumed that the hotspots were collinear, whereas the analysis of Section 5 showed that this is only approximately correct. We have therefore repeated the analysis of Section 4 but have assumed that the source components are misaligned to the extent derived in Section 5. In this analysis there is no longer any advantage in using the variable x and so we revert to the simpler quantity Q. Probability distributions of Q for the quasars and radio galaxies are shown in Fig. 10.

It is straightforward to show that, if the two hotspots move at the same non-relativistic velocity, the observed values of the non-relativistic separation quotient, Q_0, for the geometry of Fig. 8, are

$$Q_0 = \frac{1}{\sin\theta}[(\cos\phi\sin\theta + \sin\phi\cos\alpha\cos\theta)^2 + \sin^2\phi\sin^2\alpha]^{1/2}.$$

If the components move at the same relativistic velocity v,

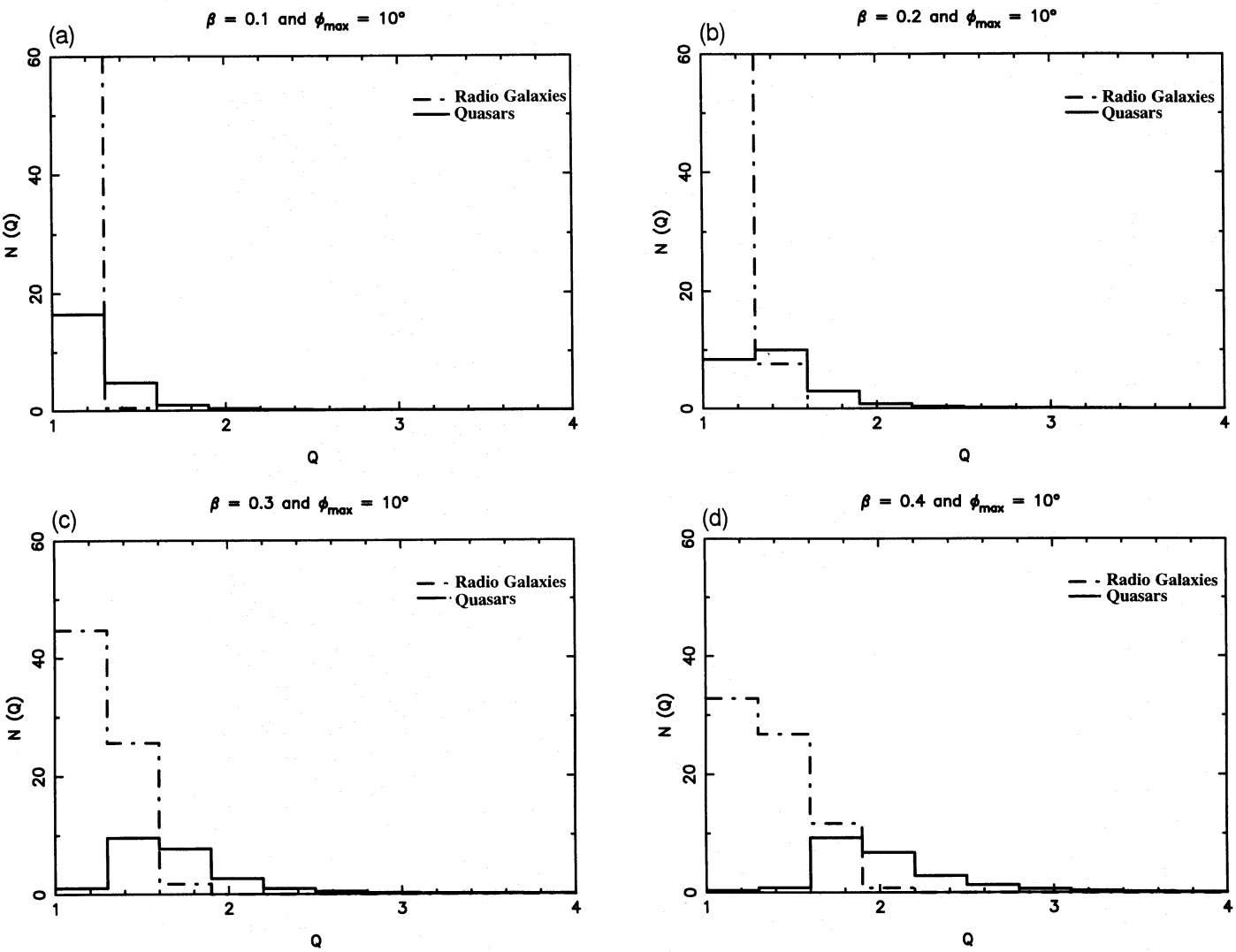

Figure 11. The predicted probability distributions for the separation quotient Q for $\phi = 10°$ and for different assumed values of $\beta = v/c$ of (a), 0.1, (b) 0.2, (c) 0.3 and (d) 0.4.

the expression for Q becomes

$$Q = \frac{[1-(v/c)\cos\theta]\,Q_0}{[1+(v/c)(\cos\theta\cos\phi+\sin\theta\sin\phi\cos\alpha)]}.$$

We have evaluated the probability distribution for the separation quotient Q for a value $\phi_{max}=10°$ and different values of the velocity of the hotspots $\beta=v/c$. The predicted distributions for values of $\beta=0.1$, 0.2, 0.3 and 0.4 are shown in Figs 11(a)–(d). It can be seen that the observed distribution of the values of Q for quasars is always somewhat broader than that of the radio galaxies, as is expected if the quasars are observed at a small angle to the line of sight and the sources are intrinsically misaligned with $\phi_{max}=10°$. It is evident from Fig. 11(a) that the observed distribution of asymmetry angles ζ cannot account for the broad distribution of the values of Q, if the velocities of the components are non-relativistic. The predicted distributions of $N(Q)$ for larger values of β, however, are broader and, in the limit of values of $\beta=0.4$, are similar to those found in the case $\phi_{max}=0°$. It is apparent from the predicted histograms that values of $\beta=0.2$–0.4 provide a much better fit to the data than the value $\beta=0$.

An alternative way of presenting these data is to fix β at a value of 0.3 and increase the value of ϕ_{max} from 0° to 30° (Figs 12a–d). It can be seen that values of ϕ_{max} of 30° result in significant numbers of quasars with small values of Q, contrary to the observations shown in Fig. 10. It is apparent that values of $\phi_{max}\sim 10°$ provide the best fit to the data.

7 THE Q–ζ DIAGRAM

The observed relation between Q and ζ for the sources in the sample is shown in Fig. 13. To illustrate the expectations of our simple model, grey-scale plots are presented in Figs 14(a)–(d), which illustrate where the quasars and radio galaxies are expected to be found in the Q–ζ diagram. The diagrams were generated using a Monte Carlo algorithm adopting the same assumptions made above, namely that the sources with $0°<\theta<45°$ are quasars and those with $45°<\theta<90°$ are radio galaxies. In all these examples, it has been assumed that $\phi_{max}=10°$. Inspection of these diagrams shows that values of $\beta\sim 0.2$–0.3 result in the types of distribution seen in Fig. 13. As expected, the quasars are concentrated towards larger values of Q, with a rather sharp

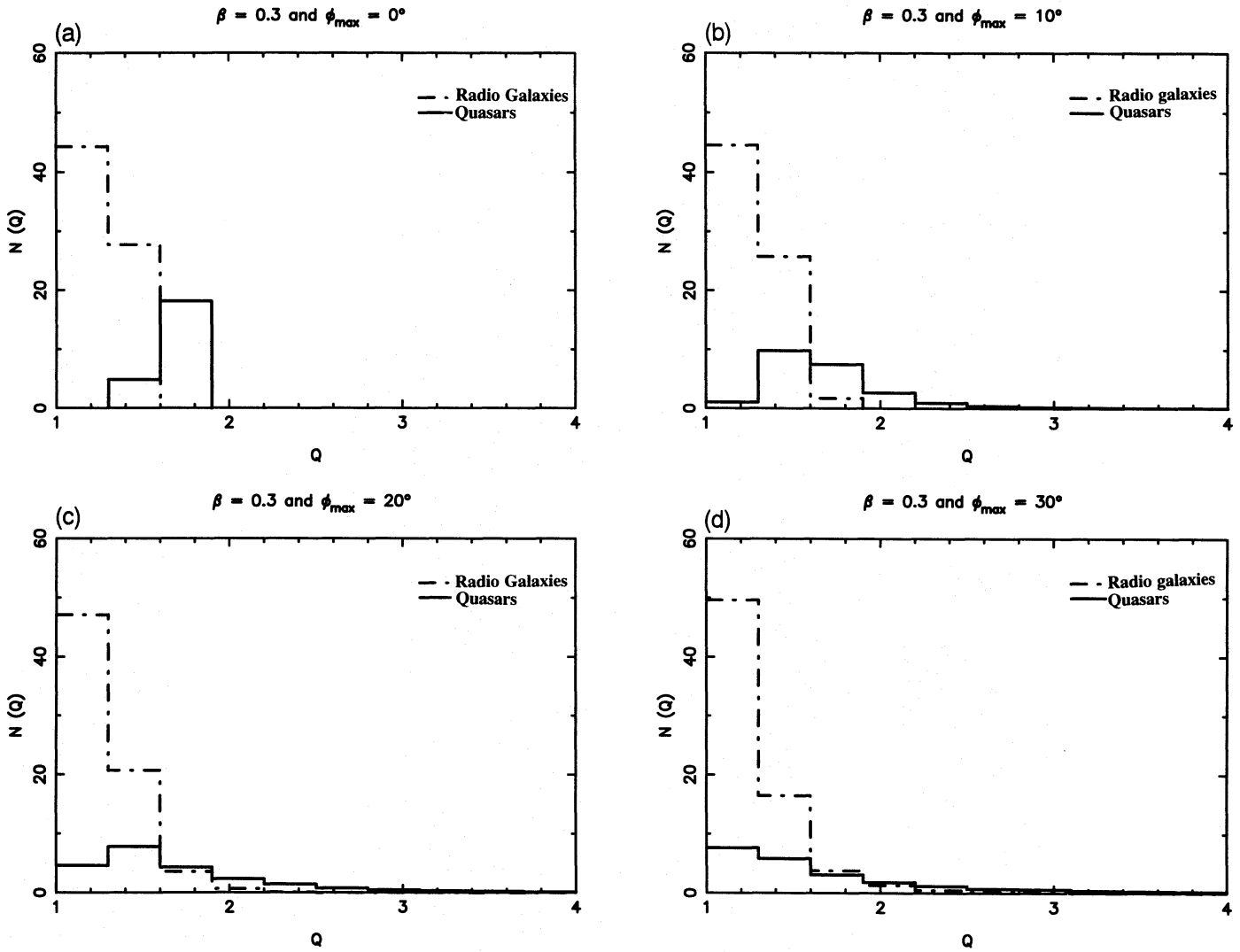

Figure 12. The predicted probability distributions for the separation quotient Q for $\beta=v/c=0.3$ and for different assumed values of ϕ_{max} of (a) 0°, (b) 10°, (c) 20° and (d) 30°.

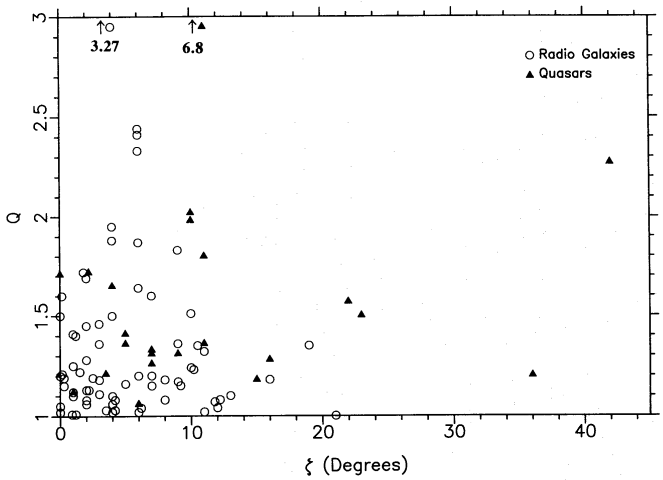

Figure 13. The observed distribution of radio galaxies and quasars in the $Q-\zeta$ diagram for the sources in the complete sample.

boundary towards lower values of Q. In contrast, the radio galaxies have a more uniform distribution, as observed.

8 DISCUSSION

Although there is considerable spread about the mean distribution, there is a clear trend for the quasars to be more asymmetric than the radio galaxies in all of the tests described above. Our conclusions are as follows.

(1) The difference in the distribution of asymmetry angles between the quasars and the radio galaxies can be attributed to the fact that all sources exhibit intrinsically the same non-collinearity, but the axes of the quasars are observed at angles closer to the line of sight than those of the radio galaxies. Our quantitative simulations show that the statistics of the asymmetry angles $\phi_{\max}$ are entirely consistent with Barthel's picture that quasars are observed when the axis of the source lies within 45° of the line of sight. This result is independent of any assumption about the velocities of the hotspots.

(2) Typically, the misalignment angles of the hotspots are randomly distributed within a cone angle $\phi_{\max} = 10°$. This angle is found by keeping one of the arms of the source fixed and allowing the other to lie randomly within this cone. If the hotspots were illuminated by jets emitted with random misalignment angles in opposite directions, the cone angles would correspond to about 6°–7° about the mean axis of the source in either direction.

(3) The observed distribution of asymmetry angles ζ alone cannot account for the observed distribution of separation quotients.

(4) The distribution of separation quotients for the quasars and radio galaxies can be explained if the hotspots are assumed to move away from the nucleus at mildly relativistic speeds. The typical speeds of advance of the hotspots would be about $0.2c$, but there is a considerable spread about this value, as illustrated in Fig. 2(b), which shows that they can extend to velocities of at least $0.4c$.

The fourth conclusion is perhaps the most surprising result of the present analysis and is in contrast with the conclusion of McCarthy et al. (1991) who found that the brighter emission-line region lies on the side of the shorter arm of the radio source, suggesting that environmental effects influence the separation quotient Q. McCarthy et al. quantified the asymmetry in the intensity of the emission-line gas on either side of the radio galaxy by the parameter R, defined to be the ratio of the intensities of the [O II] line emission on either side of the nucleus. Despite the fact that there is a very clear correlation between shorter arm length and the presence of more intense emission-line gas, we find that there is no evidence for any significant correlation between the value of R and separation quotient Q. This result suggests that environmental effects are not necessarily the dominant cause of the different arm lengths on either side of the nucleus.

It is quite conceivable that both environmental and relativistic effects are responsible for the observed distributions of Q and x. A combination of these effects would help explain why the observed value of $\bar{x}$ for radio galaxies is slightly greater than would be expected on the basis of the value of $\bar{x}$ for the quasars. Any intrinsic asymmetry due to environmental effects should be more clearly distinguishable in the radio galaxies since they are observed closer to the plane of the sky than the quasars. To make a complete analysis of this problem is beyond the scope of this paper. Instead, using average values, if an intrinsic asymmetry of $\bar{x} \approx 0.066$ were associated with environmental effects, with the remaining $\bar{x}_{\rm Q} \approx 0.140$ and $\bar{x}_{\rm RG} \approx 0.058$ being attributed to light traveltime across the source, the predicted ratio of $\bar{x}_{\rm Q}/\bar{x}_{\rm RG} \approx 2.41$ for light traveltime effects would be obtained. In this picture, the contributions from the two effects to the asymmetry of radio galaxies would be roughly equal, whilst in quasars the asymmetry would still be dominated by the light traveltime across the source. Thus there would be a correlation between short arm length and greater line emission in radio galaxies, as observed by McCarthy et al., but in quasars this should be only very weak. The reduced importance of the relativistic effect would slightly reduce the mean speeds of advance of the hotspots to $\beta \approx 0.16$.

It is interesting that independent evidence for such velocities has been found by Liu, Pooley & Riley (1992) for radio galaxies with redshifts $z \gtrsim 0.3$ (see also Laing 1993). The hotspot advance speeds were determined from synchrotron-loss ageing arguments, using equipartition magnetic field strengths, and had an average value of $\beta \approx 0.15$ with considerable scatter about the mean. It is also important that Liu et al found that the velocities of those radio galaxies with redshifts $z < 0.3$ are generally lower, $\beta < 0.1$. Interpreted literally, this would imply that, in the lower radio luminosity galaxies, the separation quotients reflect intrinsic effects rather than those associated with the mildly relativistic motion. A small proportion of the radio galaxies in our sample with redshifts $z < 0.3$ are broad-line radio galaxies. It has been suggested that broad-line radio galaxies may be the low-luminosity equivalent of the quasar population; this would eliminate the problem encountered by unified schemes in that there are no quasars at the lowest redshifts in the 3CR catalogue. These broad-line galaxies have values of x that are indistinguishable from those of the narrow-line galaxies. The hotspot advance velocities derived by Liu et al. for these lower radio luminosity sources provide a natural explanation for this observation, as intrinsic effects would be expected to dominate. It should be noted that, if these few broad-line radio galaxies were, in fact, classified separately from the narrow-line radio galaxies, there would be negligible changes to the mean

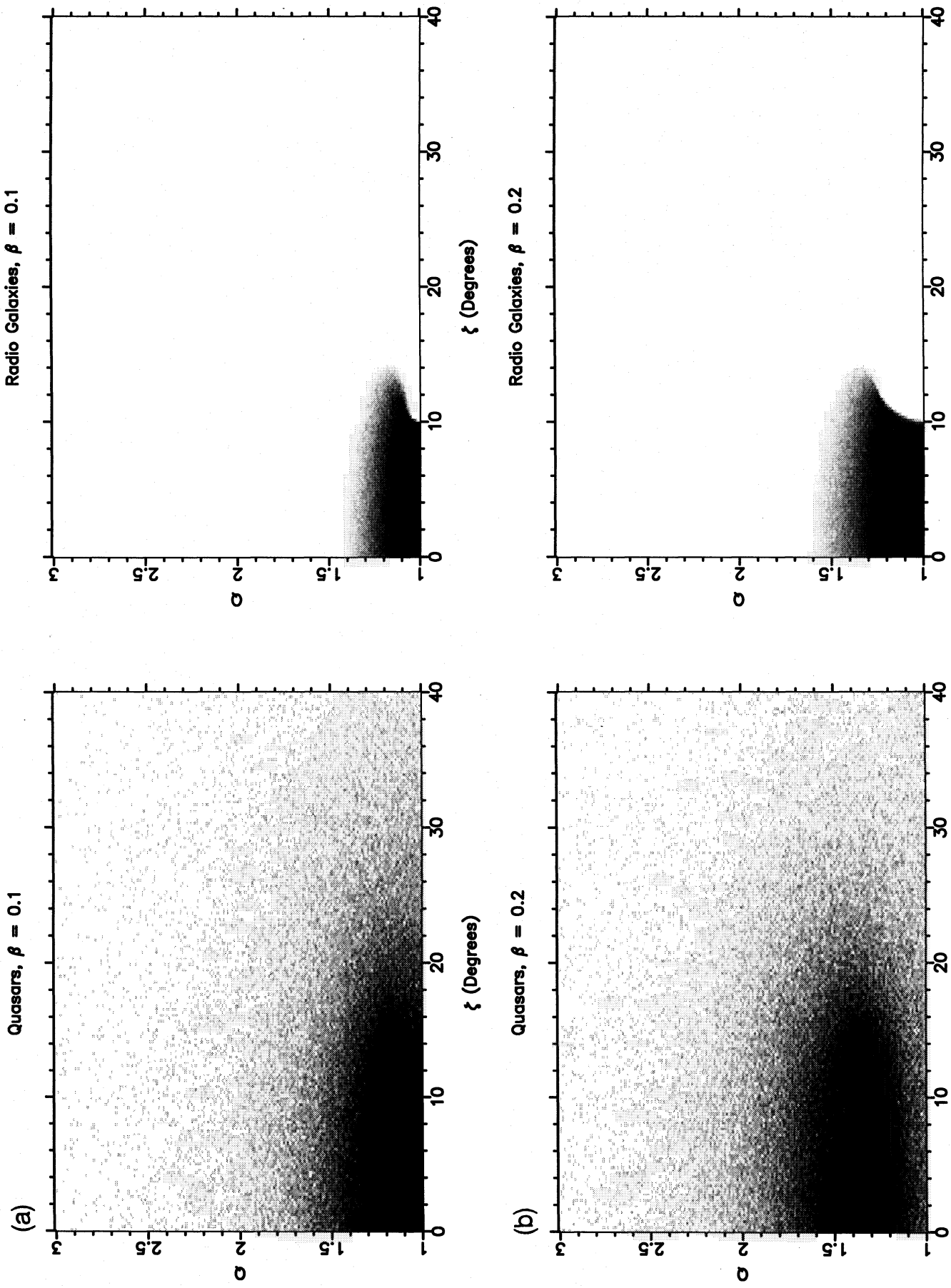

Figure 14. The predicted distribution of radio galaxies and quasars in the Q–ζ diagram for $\phi_{max} = 10°$ and for assumed hotspot velocities of (a) 0.1, (b) 0.2, (c) 0.3 and (d) 0.4.

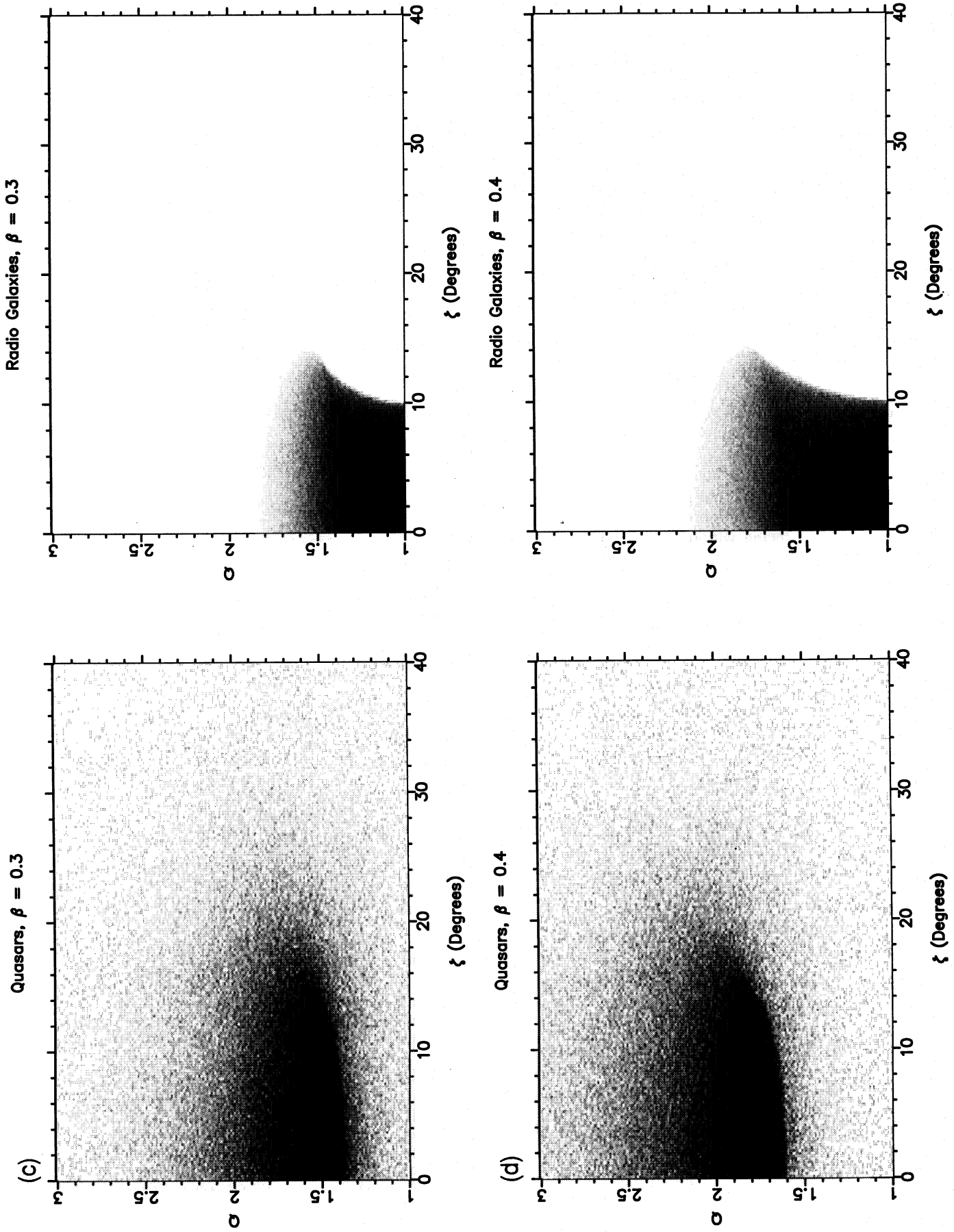

Figure 14 – *continued*

values of x, ζ and D in the remaining population of radio galaxies, and the results presented in this paper would be unaffected.

Laing et al. (1994) have suggested that low-excitation radio galaxies, generally at low redshifts, may form an isotropic sample not unified with high-excitation radio galaxies and quasars, but instead possibly forming part of the parent population of BL Lac objects. If true, this would further explain the excess of radio galaxies over quasars at redshifts $z \lesssim 0.3$. Our data are insufficient to investigate this theory.

The second conclusion can be used to make an alternative estimate of the speed of the hotspots through the intergalactic medium. If it is assumed that the jets are collinear when emitted from the nucleus, and that the asymmetry angle is associated with the motion of the parent galaxy through the intergalactic medium, the speed of advance of the hotspots can be found. As in the case of the radio-trail sources, it can be assumed that the typical velocities of galaxies in cluster environments are about 1000 km s^{-1} and so, by geometry, the speed of the hotspot would be $v_{HS} \approx 10\,000$ km $s^{-1} \approx 0.03c$. This velocity is somewhat smaller than the velocities inferred from the analysis of Section 4. It should also represent an upper limit since radio galaxies are frequently observed to be the dominant galaxy in the cluster centre, and would therefore have lower than average velocities relative to the intergalactic gas.

It might seem contrived to suppose that the jets powering the radio sources are ejected within a cone of angle 7° at almost precisely the same relativistic speeds in opposite directions. On the other hand, a similar physical situation occurs in the remarkable Galactic source SS433, in which the velocities of the jets are always $0.26c$ in opposite directions. The beams precess about the axis of the source with a cone angle of 20°, somewhat greater than the value of $\phi_{max} = 7°$ found in the above analysis. The time-scales and physical sizes associated with SS433 are many orders of magnitude smaller than those associated with the extragalactic radio sources, but the physical similarities between them are none the less striking.

Throughout our analysis, we have taken no account of the effects of relativistic beaming upon the intensities of the hotspots. The flux densities of the hotspots constitute only a small fraction of the total flux density of a typical radio source and so relativistic beaming would have only a very small effect upon the total intensity of the radio sources.

ACKNOWLEDGMENTS

The National Radio Astronomy Observatory is operated by AURA, Inc., under co-operative agreement with the National Science Foundation. We are particularly grateful to Dr Ian Browne for drawing our attention to the paper by Banhatti and for his interest in this work. Dr R. Spencer kindly provided a summary of recent information about SS433. We are grateful to the referee for pointing out an important error in our analysis. PNB acknowledges support from PPARC.

REFERENCES

Akujor C. E., Spencer R. E., Zhang F. J., Davies R. J., Browne I. W. A., Fanti C., 1991, MNRAS, 250, 215 (ASZD)
Alexander P., Leahy J. P., 1987, MNRAS, 225, 1 (AL)
Antonucci R. R. J., 1989, ApJS, 59, 499 (A)
Bailer D. M., 1993, MPhil Dissertation, University of Cambridge
Banhatti D. G., 1980, A&A, 84, 112
Barthel P. D., 1989, ApJ, 336, 606
Barthel P. D., 1994, in Bicknell G. V., Dopita M. A., Quinn P. J., eds, The First Stromlo Symposium: Physics of Active Galaxies. Cambridge Univ. Press, Cambridge, p. 175
Barthel P. D., Miley G. K., 1988, Nat, 333, 319
Barthel P. D., Miley G. K., Schilizzi R. T., Lonsdale C. J., 1988, A&AS, 73, 515 (BMSL)
Baum S. A., Heckman T., Bridle A., van Breugel W. J. M., Miley G., 1988, ApJS, 68, 643 (BHBV)
Black A. R. S., Baum S. A., Leahy J. P., Perley R. A., Riley J. M., Scheuer P. A. G., 1992, MNRAS, 256, 186 (BBLP)
Burns J. O., Christiansen W. A., Hough D. H., 1982, ApJ, 257, 538 (BCH)
Burns J. O., Basart J. P., De Young D. S., Ghiglia D. C., 1984, ApJ, 283, 515 (BBYG)
Chambers K. C., Miley G. K., Joyce R. R., 1988, ApJ, 329, L75 (CMJ)
Clarke D. A., Bridle A. H., Burns J. O., Perley R. A., Norman M. L., 1992, ApJ, 385, 173 (CBBP)
Fernini I., Burns J. O., Bridle A. H., Perley R. A., 1993, AJ, 105, 1690 (FBBP)
Fokker A. D., 1986, A&A, 156, 315
Gregorini L., Padrielli L., Parma P., Gilmore G., 1988, A&AS, 74, 107 (GPPG)
Hintzen P., Ulverstad J., Owen F., 1983, AJ, 88, 709 (HUO)
Hough D. H., Readhead A. C. S., 1989, AJ, 98, 1208
Jägers W., 1986, PhD thesis, Leiden University (J86)
Jägers W., 1987, A&AS, 71, 603 (J87)
Jenkins C. J., Pooley G. G., Riley J. M., 1977, Mem. R. Astron. Soc., 84, 61 (JPR)
Kapahi V. K., 1990, Curr. Sci., 59, 561
Kapahi V. K., Saikia D. J., 1982, JA&A, 3, 465
Laing R. A., 1989, in Meisenheimer K., Röser J.-H., eds, Hotspots in Extragalactic Radio Sources. Springer-Verlag, Heidelberg (L89)
Laing R. A., 1993, in Burgarella D., Livio M., O'Dea C. P., eds, Astrophysical Jets. Cambridge Univ. Press, Cambridge, p. 95
Laing R. A., Riley J. M., Longair M. S., 1983, MNRAS, 204, 151 (LRL)
Laing R. A., Jenkins C. R., Wall J. V., Unger S. W., 1994, in Bicknell G. V., Dopita M. A., Quinn P. J., eds, The First Stromlo Symposium: Physics of Active Galaxies. Cambridge Univ. Press, Cambridge, p. 201.
Leahy J. P., Williams A. G., 1984, MNRAS, 210, 929 (LW)
Leahy J. P., Perley R. A., 1991, AJ, 102, 537 (LP)
Leahy J. P., Muxlow T. W. B., Stephens P. W., 1989, MNRAS, 239, 401 (LMS)
Liu R., Pooley G. G., Riley J. M., 1992, MNRAS, 257, 545 (LPR)
Longair M. S., 1975, MNRAS, 173, 309 (L75)
Longair M. S., Riley J. M., 1979, MNRAS, 188, 625
Lonsdale C. J., Barthel P. D., 1987, AJ, 94, 1487 (LB)
Lonsdale C. J., Morrison I., 1983, MNRAS, 203, 833 (LM)
McCarthy P. J., van Breugel W. J. M., Kapahi V. K., 1991, ApJ, 371, 478
Owen F. N., Puschell J. J., 1984, AJ, 89, 932 (OP)
Pedelty J. A., Rudnick L., McCarthy P. J., Spinrad H., 1989, AJ, 98, 1232 (PRMS)
Perley R. A., Taylor G. B., 1991, AJ, 101, 1623 (PT)
Pooley G. G., Henbest S. N., 1974, MNRAS, 169, 477 (PH)
Ryle M., Longair M. S., 1967, MNRAS, 136, 123
Spangler S. R., Myers S. T., Pogge J. J., 1984, AJ, 89, 1478 (SMP)
Spencer R. E. et al., 1991, MNRAS, 250, 225 (SSFF)
Stocke J. T., Burns J. O., Christiansen W. A., 1985, ApJ, 299, 799 (SBC)
van Breugel W. J. M., Jägers W., 1982, A&AS, 49, 529 (vBJ)

APPENDIX

The values of the separation quotient Q given in Table A1 are generally in good agreement with the values published by McCarthy, van Breugel & Kapahi (1991). Typically, the estimates agree within ± 0.1 but there are significant discrepancies for 11 sources, which are listed in Table A2.

The differences from our adopted values are believed to be due to the following causes.

3C 13: this discrepancy is due to an error in the position of the optical galaxy on the map used by McCarthy et al.

3C 55: the map published by Leahy et al. (1989) indicates a value of Q smaller than 1.48.

3C 205: the southern component of this source is double. Our value was obtained using the more distant, slightly fainter, hotspot.

3C 215: all maps we have found are consistent with our value.

3C 223: the map by van Breugel & Jägers (1982) has a poorly defined southern hotspot. The map published by Leahy & Perley (1992) gives a much improved position for the hotspot.

3C 252, 3C 277.2 and 3C 441: our new VLA observations have provided much more accurate values of Q for these sources.

3C 299: the map published by Liu, Pooley & Riley (1992) shows that the value of Q is greater than 3.0.

3C 303 and 3C 427.1: the maps used by McCarthy et al. do not show radio cores and so the optical positions were used by them. The maps available to us had well-defined radio cores leading to more accurate values of Q.

Table A1. The properties of the radio sources.

Source	Q	x	(ζ/degrees)	(Linear Size / kpc)	(Radio Luminosity / 10^{27} W Hz^{-1})	Q/RG	Redshift	Reference
3C6.1	1.1	0.05	13	215	49.0	RG	0.840	PH
3C9	1.06	0.03	6	114	616.6	Q	2.012	LB
3C13	1.2	0.09	6	240	141.0	RG	1.351	BLRR
3C14	1.8	0.29	11	205	131.0	Q	1.469	JPR
3C20	1.04	0.02	12	202	6.20	RG	0.174	LEA
3C22	1.28	0.13	2	206	58.1	RG	0.938	BLRR
3C33	1.22	0.10	1.5	397	0.93	RG	0.059	LP
3C33.1	1.70	0.26	2	888	2.02	RG	0.181	vBJ
3C34	1.08	0.04	4	381	34.9	RG	0.690	BLRR
3C41	1.13	0.06	2	189	30.8	RG	0.795	L89
3C42	1.03	0.01	4	178	9.36	RG	0.395	LP
3C46	1.64	0.24	6	1123	11.3	RG	0.437	GPPG
3C47	1.22	0.10	3.5	456	26.1	Q	0.425	PH
3C55	1.04	0.02	6	572	71.4	RG	0.735	LMS
3C61.1	1.23	0.10	10	738	5.25	RG	0.186	LP
3C68.1	1.26	0.11	7	447	112.1	Q	1.238	LMS
3C68.2	1.12	0.06	1	189	183.9	RG	1.575	BLRR
3C79	1.32	0.14	11	433	10.2	RG	0.256	SMP
3C98	1.18	0.08	8	264	0.21	RG	0.031	BHBV
3C109	1.07	0.03	12	500	10.3	RG	0.306	A
3C153	1.6	0.23	0	44	5.67	RG	0.277	LM
3C171	1.03	0.01	3.5	171	5.56	RG	0.238	B
3C173.1	1.21	0.10	0	324	6.71	RG	0.292	LP
3C175	1.36	0.15	11	391	62.3	Q	0.768	T
3C184.1	1.35	0.15	10.5	473	0.88	RG	0.119	LP
3C190	1.57	0.22	22	57	135.5	Q	1.197	SSFF
3C191	1.71	0.26	2	40	361.5	Q	1.952	BMSL
3C192	1.19	0.09	2.5	308	0.36	RG	0.060	BHBV
3C196	1.3	0.13	9	83	281.8	Q	0.871	LM
3C204	1.41	0.17	5	300	89.7	Q	1.112	L89
3C205	1.33	0.14	7	153	185.9	Q	1.534	BBYG
3C208	1.31	0.13	7	94	130.9	Q	1.109	BBYG
3C212	1.12	0.06	1	77	101.5	Q	1.049	ASZD
3C215	2.27	0.39	42	384	10.8	Q	0.411	HUO
3C219	1.02	0.01	11	718	6.09	RG	0.174	CBBP
3C220.1	1.25	0.11	1	229	33.1	RG	0.610	BBYG
3C223	1.08	0.04	2	960	1.32	RG	0.137	LP
3C228	1.15	0.07	0	332	38.1	RG	0.552	BBYG
3C234	1.36	0.15	9	438	5.31	RG	0.185	BBYG
3C236	1.71	0.26	2	5930	0.66	RG	0.099	J87
3C239	1.87	0.30	6	93	331.0	RG	1.781	LPR
3C241	1.35	0.15	19	8	208.9	RG	1.617	ASZD
3C244.1	1.15	0.07	9	352	19.2	RG	0.428	JPR
3C249.1	2.02	0.34	10	134	5.23	Q	0.311	BBYG
3C252	1.83	0.29	9	513	89.7	RG	1.105	BLRR
3C254	6.8	0.74	15	105	63.1	Q	0.734	OP
3C263	1.71	0.26	0	345	34.8	Q	0.652	T

Table A1 – *continued*

Source	Q	x	(ζ/ degrees)	(Linear Size / kpc)	(Radio Luminosity / 10^{27} W Hz^{-1})	Q/RG	Redshift	Reference
3C263.1	1.16	0.07	5	56	70.1	RG	0.824	LPR
3C265	1.51	0.20	10	641	76.9	RG	0.811	FBBP
3C266	1.1	0.05	4	37	121.9	RG	1.272	BLRR
3C267	1.19	0.09	0	326	119.0	RG	1.144	BLRR
3C268.4	1.18	0.08	15	93	116.3	Q	1.400	LM
3C270.1	1.20	0.09	36	102	174.3	Q	1.519	SBC
3C274.1	1.05	0.02	0	986	15.5	RG	0.422	LW
3C275.1	1.50	0.20	23	133	31.9	Q	0.557	SBC
3C277.2	2.41	0.41	6	472	43.3	RG	0.766	BLRR
3C280	1.18	0.08	3	123	127.4	RG	0.996	LPR
3C284	1.41	0.17	1	831	3.30	RG	0.239	B
3C285	1.18	0.09	16	268	0.34	RG	0.079	AL
3C289	1.02	0.01	4	84	62.7	RG	0.967	BLRR
3C292	1.15	0.07	7	1060	27.3	RG	0.710	AL
3C295	1.40	0.17	1	36	86.0	RG	0.461	PT
3C299	3.27	0.53	4	70	7.73	RG	0.367	LPR
3C300	2.33	0.40	6	516	6.57	RG	0.272	B
3C303	1.00	0.00	1	139	1.07	RG	0.141	LP
3C321	1.13	0.06	2	687	0.58	RG	0.096	LW
3C322	1.2	0.09	0	278	169.7	RG	1.681	JPR
3C324	1.6	0.23	7	86	141.1	RG	1.206	FBBP
3C330	1.0	0.00	0	457	42.3	RG	0.549	LMS
3C334	1.65	0.25	4	812	18.1	Q	0.555	T
3C336	1.98	0.33	10	183	51.9	Q	0.927	T
3C337	1.88	0.31	4	333	23.3	RG	0.635	PRMS
3C340	1.06	0.03	2	384	31.6	RG	0.775	BLRR
3C341	1.2	0.09	7	474	11.4	RG	0.448	JPR
3C349	1.06	0.03	4	352	2.72	RG	0.205	LP
3C351	1.36	0.15	5	402	9.36	Q	0.371	LP
3C356	1.50	0.20	0	640	86.6	RG	1.079	FBBP
3C368	1.98	0.33	4	67	138.8	RG	1.132	CMJ
3C381	1.11	0.05	3	247	2.10	RG	0.161	H
3C382	1.08	0.04	12	287	0.31	RG	0.058	A
3C388	1.00	0.00	21	97	0.96	RG	0.091	BCH
3C390.3	1.45	0.18	2	318	0.70	RG	0.056	LP
3C427.1	1.24	0.11	10	172	49.5	RG	0.572	L89
3C432	1.28	0.12	16	108	256.6	Q	1.805	T
3C436	1.20	0.09	6	461	4.10	RG	0.215	H
3C437	1.10	0.05	1	294	184.0	RG	1.480	BLRR
3C438	1.17	0.08	9	118	19.2	RG	0.290	LP
3C441	2.44	0.42	6	255	34.4	RG	0.708	BLRR
3C452	1.02	0.01	6	511	1.70	RG	0.081	BBLP
3C457	1.08	0.04	8	1258	13.3	RG	0.428	LP
3C469.1	1.0	0.00	1	634	130.4	RG	1.336	L75
3C470	1.36	0.15	3	203	157.5	RG	1.653	BLRR
4C14.11	1.46	0.19	3	379	2.33	RG	0.206	LP
4C14.27	1.5	0.20	4	216	9.05	RG	0.392	LP
4C73.08	1.20	0.09	0	1441	0.23	RG	0.058	J86

The initials in the final column of the table correspond to references in the reference list, with the following exceptions: BLRR – Best P. N., Longair M. S., Röttgering H. J. A., Riley J. M. (in preparation); B – Blundell K. (private communication); H – Hardcastle M. (private communication); LEA – Leahy J. P. (private communication); T – Turner S. (private communication).

Table A2. Sources with discrepant values of Q.

Source	Q(this paper)	Q(McCarthy et al)
3C13	1.2	2.22
3C55	1.04	1.48
3C205	1.33	1.15
3C215	2.27	1.78
3C223	1.08	1.25
3C252	1.83	2.0
3C277.2	2.41	2.69
3C299	3.27	3.00
3C303	1.00	1.84
3C427.1	1.24	1.51
3C441	2.44	3.13